2. TECHNICAL REVIEW

2.1 Variables Affecting Slurry Bubble Column (SBCR) Performance

A slurry bubble column reactor (SBCR) is usually a cylindrical vessel in which gas (containing one or more reactants, e.g. synthesis gas for FT processes) is sparged through the liquid (containing liquid reactant(s) and products), and a finely dispersed catalyst. As long as the operating liquid superficial velocity (in the range of 0 to 2 cm/s) is an order of magnitude smaller than the superficial velocity of the gas (1 to 30 cm/s), and the catalyst particles are small (less than 50 μm) and not excessively heavy, the gas dominates the hydrodynamics and, by buoyancy forces resulting from the nonuniform cross-sectional gas holdup distribution induces liquid velocities order of magnitude larger than the liquid superficial velocity. The finely dispersed catalyst follows the motion of the liquid.

Interpretation of SBCR performance must rely on an appropriate model which properly accounts for the events on the molecular scale (e.g. kinetics and catalyst particle performance, etc.), micro-scale (e.g. transport of reactants and products to and from the catalyst particle and of reactants from gas bubbles to the liquid) and macro-scale (e.g. liquid backmixing) on heat transfer and reactor performance. We know that numerous design and operating variables, listed in Figure 2.1, and physicochemical and thermodynamic properties of the fluid affect the many highly interactive phenomena in SBCR. All of these in turn affect reactor performance.

A slurry bubble column reactor for FT synthesis and other syngas processes in order to be economically successful, must operate at high volumetric productivity which requires high activity catalyst, high catalyst loading of the slurry, large gas flow rate and high gas conversion. The ability to achieve complete catalyst suspension and the desired flow pattern (degree of backmixing) of the liquid phase are crucial to the targeted reactor performance. In order to accomplish these an improved understanding and quantification of the key hydrodynamic phenomena is required.

We focus here our attention on properly describing the liquid (slurry) circulation and turbulence in SBCR for Fischer Tropsch synthesis because it is the liquid mixing that affects catalyst distribution, bubble coalescence, gas-liquid interfacial area, mass transfer coefficients and heat transfer from the reactor. We first summarize our current understanding of flow regimes and gas holdup, and their effect on liquid backmixing.

Flow regime affects gas holdup and holdup distribution. The available standard flow maps (e.g. Shah et al., 1982) are old and not very reliable in identifying the flow regime in FT SBCRs. It is commonly assumed, based on evidence of multiple bubble sizes (Patel et al., 1990; De Swart, 1996), that churn-turbulent flow occurs in FT waxes at superficial gas velocities above 5 cm/s. This needs additional verification. Information on characteristic bubble size as well as reliable diagnostic of the flow regime are needed.

Gas holdup is the fraction of the column occupied by gas. As Fan (1989) illustrates, existing older correlations cannot predict holdup accurately and no agreement regarding holdup is reached for Fischer Tropsch waxes (Quicker and Deckwer, 1981). Kemoun *et al.* (2000) studied the effect of pressure on gas holdup and its cross-sectional distribution using γ-ray Computed Tomography (CT) in air-water system at elevated pressures up to

0.7 MPa. The cross-sectional average gas holdup was calculated using the collected data and compared with various correlations found in the literature. Their main findings are:

- At atmospheric pressure, the correlation of Idogawa *et al.* (1985) was in the best agreement with experimental data except for U_G = 0.05 m/s. This operating condition is near the transition point, and the correlation and data may not belong to the same flow regime.
- At higher pressures and over the entire superficial gas velocity range investigated (2 to 30 cm/s), the correlation of Hammer *et al.* (1984) gives the best prediction of gas holdup data (average error of 12-17%) followed by Wilkinson *et al.* (1992; average error of 14-18%) and Idogawa *et al.* (1987; average error of 18-20%).
- At higher pressures and high superficial gas velocity ($U_G > 0.1$ m/s), in addition to the correlations of Idogawa *et al.* (1987), and Hammer *et al.* (1984), the correlation of Krishna *et al.* (1996) and Luo *et al.* (1999) also seem to provide reasonable predictions of the measured gas holdup.

They also concluded that they were not able to find any correlation that consistently predicted their experimental data well under all process conditions, which indicates the need for better characterization of the levels of liquid recirculation and turbulence which are needed for development of a more fundamentally based model for prediction of gas holdups (Fan, 1989).

Radial gas holdup distribution drives liquid recirculation as originally shown by Hills (1974). This distribution depends on operating conditions, physical properties of the system and distributor type (e.g. Chen et al., 1999; Rice and Geary, 1990). It has not been determined in FT SBCRs.

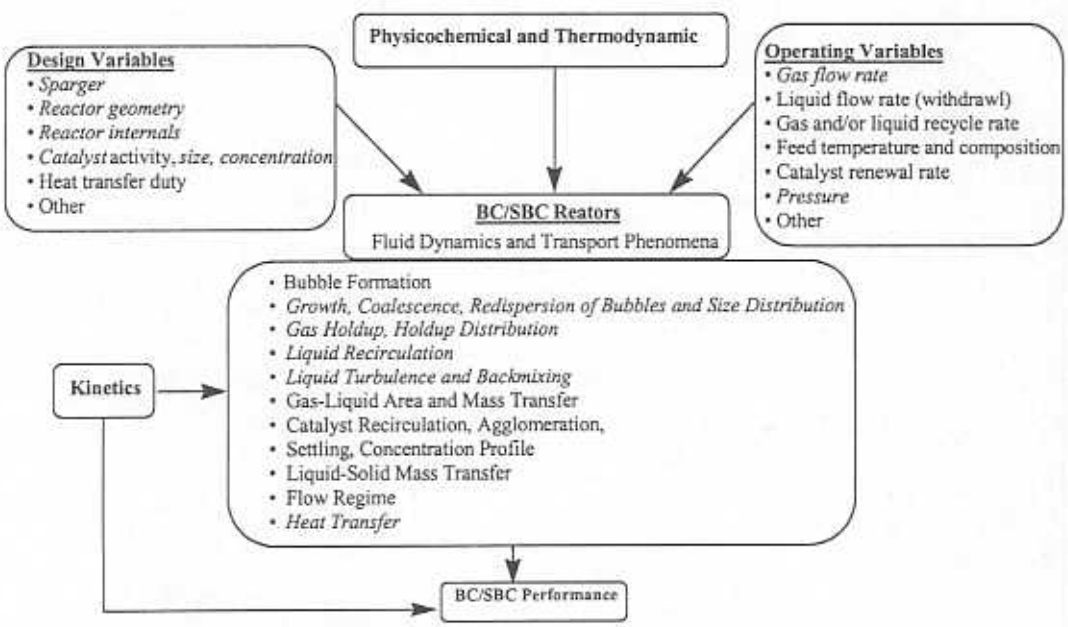

Figure 2.1: Variables that affect SBCR performance

Quantification of liquid backmixing is essential for reactor design, scale-up and interpretation of reactor performance. This is most commonly done by the use of the axial dispersion model. Fan (1989) compares the predictions for the liquid axial dispersion coefficient obtained from various correlations at different gas velocities and in columns of different diameter for the air-water system. The agreement leaves a lot to be desired, which is not surprising since the model assumes a flat velocity profile with eddy axial dispersion superimposed on it. However, the axial liquid velocity profile in a bubble column is anything but flat and, therefore, the axial dispersion coefficient has to account for a variety of mixing mechanisms, including non-uniform velocity, convective transport, bubble wake turbulence, liquid axial and radial turbulence, etc. The dominant mixing mechanism is due to liquid recirculation with contribution from wake and eddy dispersion. Therefore, the correlations reported in the literature, and summarized by Fan (1989), form a poor basis for design/scale-up.

Recently, Degaleesan (1997) has shown that the effective axial dispersion coefficient can be related to liquid recirculation and radial eddy diffusivity via Taylor type diffusivity and to the axial eddy diffusivity. She proposed a scale-up procedure to estimate the fluid dynamic parameters of industrial systems needed for prediction of their performance. The validity of the model proposed by Degaleesan (1997) for evaluation of these parameters on FT systems needs experimental verification.

Liquid recirculation in bubble columns (BC) has been observed and documented by Hills (1974), Rice and Geary (1990) and Devanathan (1991). A novel noninvasive experimental technique, based on monitoring the motion of a single radioactive particle, was used to demonstrate (Devanathan, 1991; Degaleesan 1997) that multiple stationary circulation cells, as proposed by Joshi and Sharma (1979), do not exist. Some preliminary data on slurry recirculation has been reported by Sannaes et al. (1995), Grevskott et al. (1996) and Rados (1999). Additional data in more concentrated slurries is needed.

Mean bubble size and bubble size distribution are also important parameters for SBCR performance, which depends on the flow regime and properties of the system. Insufficient information exists for SBCR in general and for FT systems in particular in spite of the recent work by de Swaart (1996).

2.2 Some aspects of bubble dynamics and hydrodynamic properties

The critical review of high-pressure phenomena of bubbles in liquid and liquid-solid suspension is discussed in Appendix A attached (Fan, et al., 1999). In this section some aspects of bubble dynamics and hydrodynamic properties that are reported in Appendix A are summarized.

2.2.1 Bubble Dynamics

Single bubble rise velocity

In liquid-solid suspensions under elevated pressure and temperature conditions, the bubble rise velocity is discussed in light of both the apparent homogeneous (or effective) properties of the suspension and the recently evolved numerical prediction based on a computational model for gas-liquid-solid fluidization systems. In the literature, it is found that the single bubble rise velocity does not depend on the gas density over the range of

0.1 to 30 kg/m^3. The effects of pressure and temperature, or more directly, the effects of physical properties of the gas and liquid phases on the variation of bubble rise velocity (u_b) with bubble diameter (d_b) could be represented or predicted most generally by the Fan-Tsuchiya equation (Fan and Tsuchiya, 1990) among three predictive equations. The other two are the modified Mendelson's wave-analogy equation (Mendelson, 1967) and a correlation proposed by Tomiyama et al. (1995).

In general, the bubble rise velocity decreases with an increase in pressure for a given solids holdup. A more drastic reduction in u_b can arise from the addition of solid particles. While the particle effect is small at low solids holdup, the effect is appreciable at high solids holdup, especially for high liquid viscosity. The reduction of the bubble rise velocity with an increase in pressure can lead to a significant increase in the gas holdup of three-phase fluidized beds. By comparing the pressure effect on the gas holdup with that on the bubble rise velocity, the increase in gas holdup with pressure is a consequence of the decreases in both the bubble size and the bubble rise velocity.

Heterogeneous approach: Discrete-phase computation

A two-dimensional discrete-phase simulation model for gas-liquid-solid fluidization systems has been developed recently (Jean and Fan, 1990; Luo, et al., 1997; Zhang et al., 1998a,b) to provide a much more thorough scheme of prediction of a single bubble rising in a liquid-solid fluidized bed. In this model, the volume-averaged method, the dispersed particle method (DPM) and the volume-of-fluid (VOF) method are used to account for the flow of liquid, solid, and gas phases, respectively. A bubble induced force (BIF) model, a continuum surface force (CSF) model, and Newton's third law are applied to account for the couplings of particle-bubble (gas), gas-liquid, and particle-liquid interactions, respectively. A close distance interaction (CDI) model is included in the particle-particle collision analysis, which considers the liquid interstitial effects between colliding particles.

The motion of a particle in a flow field can be described in Lagrangian coordinates with its origin attached to the center of the moving particle. The motion of a single particle can be described by its acceleration and rotation in a nonuniform flow field. The forces acting on a particle include interface forces between the fluid and particle, and forces imposed by external fields. The total force acting on a particle is composed of all applicable forces, including drag, added mass, gravity/buoyancy, Magnus force, Basset force, and other forces. The general scheme of a stepwise molecular dynamic (MD) simulation (Tildesley, 1987), based on a predictor-corrector algorithm, is used to compute the particle motion. The hard sphere approach is used for the collision dynamics. The collinear collision model is used to determine the normal velocity and momentum changes of colliding particles. The model includes the detailed close-range particle-fluid and particle-particle interactions during the entire process of particle collision. The tangential velocity and momentum changes are formulated and calculated based on a sticking/sliding model (Zhang et al., 1998a).

Bubble formation, initial bubble size, and jetting

Among various factors that affect the bubble formation, the wettability of the orifice surface is an important factor, which affects the initial size of the bubble formed on the

orifice. It is found that initial bubble size increases significantly with the contact angle between the bubble and the orifice surface when the contact angle exceeds the threshold value of 45°. The high-pressure studies indicated that an increase in gas density reduces the size of bubbles formed from a single orifice. A mechanistic model is described to predict the initial bubble size in liquid-solid suspensions at high-pressure conditions (Luo, et al., 1998c). The model considers various forces induced by the particles. During the expansion and detachment stages, particles collide with the bubble and stay on the liquid film. The particles and the liquid surrounding the bubble are set in motion as the bubble grows and rises. The model is applied to simulate the bubble formation process under constant flow conditions, which are characterized by constant gas flow rate through the orifice. When the volume of the gas chamber is small, the bubble formation can normally be assumed under constant flow conditions.

Bubble coalescence

For gas-liquid systems, the experimental results available in the literature indicate that an increase of pressure retards the bubble coalescence. It is known that surface tension decreases and liquid viscosity increases with increasing pressure. In addition, particle sphericity ϕ increases with pressure. These variations contribute to the reduction of the film thinning velocity, and hence, the bubble coalescence rate, as pressure increases. As a result, the time required for two bubbles to coalesce is longer and hence the rate of overall bubble coalescence in the bed is reduced at high pressures. Moreover, the frequency of bubble collision decreases with increasing pressure. An important mechanism for bubble collision is bubble wake effects (Fan and Tsuchiya, 1990). When the differences in bubble size and bubble rise velocity are small at high pressures, the likelihood of small bubbles being caught and trapped by the wakes of large bubbles decreases. Therefore, bubble coalescence is suppressed by the increase in pressure, due to the longer bubble coalescence time and the smaller bubble collision frequency.

Bubble breakup and maximum stable bubble size

There are many models proposed in the past that predicts the maximum stable bubbles size but they all do not account for the internal circulation of the gas. The internal circulation velocity is of the same order of magnitude as the bubble rise velocity. A centrifugal force is induced by this circulation, pointing outwards toward the bubble surface. This force can suppress the disturbances at the gas-liquid interface and thereby stabilizing the interface. On the other hand, the centrifugal force can also disintegrate the bubble, as it increases with an increase in bubble size. The bubble breaks up when the centrifugal force exceeds the surface tension force, especially at high pressures when gas density is high.

An analytical criterion for the bubble breakup is derived by considering a single large bubble rising in a stagnant liquid or slurry at a velocity of u_b, without any disturbances on the gas-liquid interface. The bubble is subjected to breakup when its size exceeds the maximum stable bubble size due to the circulation-induced centrifugal force (Luo et al., 1998a).

2.2.2 *Macroscopic Hydrodynamics*

Hydrodynamic similarity

Numerous studies have been conducted to investigate the effect of pressure on the gas holdup of bubble columns and three-phase fluidized beds. Further, empirical correlations have been proposed for gas holdup in bubble columns operated at elevated pressure and temperature (Fan et al., 1999; Kemoun et al., 2000). A similarity rule has been developed to simulate the hydrodynamics of industrial reactors which requires hydrodynamic similarity of the following dimensionless groups to be the same: U_g/u_{max}, Mo_m, and ρ_g/ρ_m.

Heat transfer characteristics

A consecutive film and surface renewal model is used to analyze the heat transfer behavior. The model assumes that a thin liquid film exists surrounding the heating surface; and liquid elements are forced to contact the outer surface of the film, due to the passage of bubbles. The liquid elements contact the film for a short time, t_c, and then, are replaced by fresh liquid elements. The heat is transferred to the bulk liquid through conduction by the liquid film and unsteady state conduction by the liquid elements. The heat transfer coefficient is expressed in terms of the physical properties of the liquid, the film thickness, and the contact time of the liquid elements (Wason and Aluwalia, 1969). By considering the pressure effects on the physical properties of liquid and bubble characteristics, such as bubble size and bubble rise velocity, this model may be used to analyze the heat transfer behavior in a high-pressure system.

2.3 *Models used for FT reactor performance prediction*

The use of slurry bubble column reactors (SBCR) provides an attractive alternative to traditional vapor-phase processes. Fischer-Tropsch (FT) synthesis has been recognized as a promising method for environmentally benign, indirect, coal utilization. Advantages of the three phase slurry FT synthesis process include: nearly isothermal operation, high catalyst effectiveness factor due to the smaller catalyst particle sizes, lower rate of catalyst deactivation and low pressure drop. Hence, SBCR is the favored reactor for commercialization of FT synthesis. However, one of the disadvantages of FT SBCR is the uncertainty of its design and scale-up in addition to the need for liquid-catalyst separation, catalyst attrition, etc. In addition to the mentioned advantages, slurry FT synthesis process doesn't require high hydrogen/carbon monoxide ratio syngas compared to fluidized or fixed bed reactor processes and hence, it can use the low hydrogen/carbon monoxide ratio syngas that is produced by the new generation of coal gasifiers. The chemical reaction of the FT synthesis (Paraffin synthesis) is as follows:

$$CO + (1 + \frac{m}{2n})H_2 \longrightarrow \frac{1}{n}C_nH_m + H_2O \qquad , m=2n+2 \qquad (2.1)$$

In processes that utilize iron catalyst and/or low hydrogen/carbon monoxide inlet ratio water gas shift reaction (WGS) should also be considered (Stern et al., 1985, Prakash, 1993; van der Laan et al., 1999):

$$CO + H_2O \longrightarrow CO_2 + H_2 \qquad (2.2)$$

Detailed kinetics that is probably needed for the accurate FT process modeling should at least also include methane ($n=1$), olefin ($m=2n$) synthesis and Boudouard's reaction:

$$2CO \longrightarrow C_{(s)} + CO_2 \qquad (2.3)$$

The basic paraffin synthesis kinetics (i.e., FT synthesis kinetics) have been almost exclusively used in the published FT models. Paraffin synthesis kinetics have been found to be of a Langmuir-Hinshelwood (L-H) type (Van der Laan, et al., 1999). However at hydrogen conversion below 60 % first order hydrogen kinetics (FTS 1st) has been shown to be a reasonable approximation (Dry, 1976; Huff and Satterfield, 1984). Table 2.1 lists the kinetic types used in FT SBCR performance modeling.

Due to the lack of understanding of the hydrodynamics of churn-turbulent slurry bubble column, most of the models assumed uniform concentration of the catalyst throughout the reactor. Following the work of Kato et al. (1972) some of the models calculated the catalyst axial concentration profile by using sedimentation and dispersion model (SDM) (Deckwer et al., 1982; Mills et al., 1996). These models have shown that in spite of small particle size and churn turbulent regime solids phase concentration is the highest at the bottom of the column and exponentially drops with height for batch slurry operation. However, the profiles of solids distribution in co-current and counter-current modes of operation strongly depend on the direction and magnitude of slurry inlet velocity (Mills et al., 1996).

Fisher-Tropsch process is highly exothermic and hence, one would naturally consider modeling the energy balance. However, results of several models (Deckwer et al., 1982; Mills et al., 1996) predict nearly isothermal operation of the FT slurry reactor. Turner and Mill's (1990) model predicted a slight temperature axial gradient (with local temperature within 20% from wall temperature). They related it to catalyst concentration axial profiles (SDM). In the mentioned models, the energy balance axial convection, reaction heat, wall convection and axial dispersion are included. However, all of these models neglected latent heat of evaporation whose contribution may be expected to be appreciable.

All published models on FT process treated the solids and liquid as one pseudo homogeneous slurry phase (SL). Slurry phase is the most often modeled as completely mixed (CM) (Bukur, 1983; Maretto and Krishna, 1999; van der Laan, 1999) or using axial dispersion model (ADM) (Deckwer et al., 1982; Mills et al., 1996; De Swart et al., 1997). Leib et al. (1995) used multi cell model for both liquid (completely mixed) and gas phase (plug flow, PF) so that the extent of backmixing has been varied by changing the number of mixing cells. Turner and Mills (1990) compared the predictions of mixing cell model (MCM) and axial dispersion model (ADM) and concluded that mixing cell model is more realistic approach although both models predicted the same performance of FT slurry reactor when number of cells (MCM) and Peclet number (ADM) were matched using a proposed correlation. Gas phase (G) has been traditionally modeled as a single phase in plug flow (PF) or with axial dispersion. Last few years several models appeared that described gas phase using two bubble class approach. In this approach small bubbles phase (SB) is modeled as completely mixed (as slurry phase), while large bubbles phase

(LB) is in plug flow (Maretto and Krishna, 1999; van der Laan et al., 1999), or alternatively, both of the gas phases are modeled using ADM (De Swart et al., 1997).

Table 2.1 shows a summary of the most relevant studies on the modeling of FT slurry bubble column reactors. The stoichiometry of the Fischer-Tropsch synthesis (eq. 2.1) is such that more moles reacts than it is produced. Because of this the amount of gas phase decreases along the FT slurry reactor with experimentally determined contraction factor α of about –0.5. Because of this effect valid model of the FT process must include a closure for the superficial gas velocity (SGV) axial profile. Classical approach assumes linear relationship between SGV and conversion of syngas (Deckwer et al., 1982):

$$U_G = U_G^i(1+\alpha X_{H_2+CO}) \tag{2.4}$$

Overwhelming number of different models is adopting this relationship (Table 2.1) although strictly this is valid only in steady state when axial mixing and convection in the liquid phase can be neglected (Stern et al., 1985). More accurate, rigorous modeling of the SGV axial profile is based on the overall gas phase mass balance (Prakash, 1993; Stern et al., 1985) which requires knowledge of the concentration profiles of all gaseous species. The drawback of this approach is obviously larger number of equations that have to be solved compared to classical Deckwer's approach.

Model for the prediction of the Fischer-Tropsch slurry reactor performance is needed which properly should include detailed kinetics with all relevant species, mixing pattern of different phases (e.g., the phenomenological multi cell recirculation model (Degaleesan et al., 1997)), change in SGV, solids axial profile, (e.g., the mechanistic model (Murray and Fan, 1989)), etc. In addition the present energy balance modeling may need to be improved by accounting for the latent heat of evaporation. In order to achieve this, detailed understanding of the hydrodynamics of FT slurry bubble column reactor via advanced diagnostic techniques is needed which is the focus of the tasks set for this grant.

Table 2.1. Summary of models for prediction of the Fischer-Tropsch process performance.

Model	Kinetics	Accounted species	Phase degree of mixing	Gas velocity profile	Solids profile	Energy balance	Steady state model
van der Laan et al., 1999	FTS, L-H WGS, L-H	H_2, CO, H_2O, CO_2 n products	SB-CM LB-PF SL-CM	f(X,α)	uniform	Yes	Yes
Maretto and Krishna, 1999	FTS, L-H	H_2, CO	SB-CM LB-PF SL-CM	uniform	uniform	iso-thermal	Yes
De Swart et al., 1997	FTS, 1st	H_2	SB-AD LB-AD SL-AD	f(X,α)	SDM	Yes	dynamic
Mills et al., 1996	FTS, 1st	H_2	G-AD SL-AD	f(X,α)	SDM	Yes	Yes
Leib et al., 1995	FTS, 1st	H_2	G-nCM or nPF L-nCM	f(X,α)	uniform	iso-thermal	Yes
Prakash, 1993	FTS, L-H WGS, L-H	H_2, CO, H_2O, CO_2	G-AD SL-AD	overall gas MB	SDM	Yes	Yes
Truner and Mills, 1990	FTS, 1st	H_2	G-nCM or nPF L-nCM , G-AD L-AD	f(X,α)	SDM	Yes	Yes
Kuo, 1983	FTS, L-H WGS, L-H	H_2, CO, H_2O, CO_2	G-PF SL-PF , CMorAD	f(X,α)	uniform	iso-thermal	Yes
Stern, et al., 1985	FTS, 1st WGS, 2nd	H_2, CO H_2O, CO_2 C_nH_m	G-AD SL-AD	overall gas MB	SDM	iso-thermal	Yes
Bukur, 1983	FTS, 1st	H_2	G-PF SL-CM	f(X,α)	uniform	iso-thermal	Yes
Deckwer et al., 1982	FTS, 1st	H_2	G-AD SL-AD	f(X,α)	SDM	iso-thermal	Yes

2.4 Physical Properties of FT Systems

2.4.1 Fischer-Tropsch waxes and solvent

It is known that the hydrodynamics of Fischer-Tropsch Synthesis process is greatly affected by the fluid physical properties of the waxes. Due to the high temperature and high pressure operating conditions for Fischer-Tropsch Synthesis, it is hard to conduct experiments at the matching conditions of Fischer-Tropsch Synthesis. Therefore, other hydrocarbons with similar physical properties as Fischer-Tropsch waxes under the operating conditions have been used to simulate the actual waxes to study the hydrodynamics of Fischer-Tropsch Synthesis. Several studies have been reported in the literature about the physical properties of different Fischer-Tropsch waxes and solvents used for the mimicking purpose (Gormley, et al., 1997; Marano and Holder, 1997; Patel, et al., 1990; Soong, et al., 1997). Table 2.2 shows the reported values of Fischer-Tropsch waxes and solvents. It can be observed that the density of reported Fischer-Tropsch waxes range from 645-849 kg/m^3. The viscosity of waxes on the other hand ranges from 0.41 to

71.9 cP. In general, the viscosity of most of the waxes used is around 2 to 4 cP. The range of surface tension stays reasonably constant between 16 and 28 dyne/cm.

Other than experimental data, models have been developed to predict the physical properties of Fischer-Tropsch liquids. Tables 2.3 and 2.4 show the asymptotic behavior correlations developed by Marano and Holder (1997) to estimate the properties of n-paraffins. The molar volume information derived from the correlation can be converted into density information by dividing the molar volume with the molecular weight of the n-paraffins used.

Table 2.2. The Physical Properties of Fischer Tropsch Waxes (Gormley, et al., 1997; Marano and Holder, 1997; Patel, et al., 1990; Soong, et al., 1997).

Fischer Tropsch Wax	Temperature (°C)	Density (kg/m3)	Viscosity (cp)	Surface Tension (dyne/cm)
ACPI wax	121	-	1.7	-
Arge wax	121	-	5.7	-
	150	-	4.2	24
	200	-	2.9	20
	230	-	2.5	19
	265	-	-	16
C28H58	110	-	20	-
	130	-	19.8	-
	150	-	5.6	-
d. Allied-AC-1702	110	-	-	-
	130	-	71.9	-
	150	-	46.3	-
Drakeol-10 Oil	20	849	38.13	28.3
	100	806	3.38	23.9
	175	-	-	19.9
	200	743.9	0.892	-
	265	698	0.55	-
FT-200 Wax	150	-	4.4	-
	200	-	2.8	-
	230	-	2.4	-
	149	-	4.4	-
	204	-	2.2	-
	260	-	1.7	24
FT-300 Wax	150	-	6.4	24
	200	722	4.2	21
	230	-	-	19
	265	681	2.7	17
F-T lt. Cut	25	-	-	23
F-T med. Cut	25	-	2.36	26
	100	-	0.842	-
	150	-	0.555	-
Kogasine	145	-	0.41	18
Krupp wax	200	-	3.0	-
	230	-	2.2	-
	260	-	1.6	-
Mobil run 3	149	-	2.8	-
	204	-	1.7	-
	260	-	-	26-27
Mobil run 4	149	-	6.1	-

	204	-	4.3	-
	260	-	3.4	26-27
Mobil run 5	149	-	17.6	-
	204	-	8.5	-
	260	-	5.5	28
Mobil run 7	149	-	8.2	-
	204	-	4.1	-
	260	-	2.3	26-27
Mobil comp	150	-	6.5	-
	200	-	3.8	-
	230	-	3.1	-
Mobil Wax	121	-	9.5	-
	200	716	3.8	-
	265	674	2.3	
Mobil FT Wax	110	-	26.6	-
	130	-	19.4	-
	150	-	17.2	-
P & W wax	100	-	1.829	-
	150	-	0.995	-
Paraflint	121	-	9.5	-
Paraffin wax	145	-	13.0	29.1
	175	-	8.1	27.0
	200	-	5.7	25.2
	220	-	4.0	24.0
	250	-	2.8	21.8
	260	-	2.0	21.2
	275	-	1.8	20.4
	300	-	1.2	19.8
Polywax-655	110	-	20.6	-
	130	-	14.5	-
	150	-	10.6	-
Sasol Wax	200	701	2.9	-
	265	655	2.0	-
UCC wax	121	-	2.8	-
n-Paraffins	0-300°C	See Table 2		

Table 2.3. Temperature-Independent Parameters for Properties of *n*-Paraffins

$Y = Y_{\infty,0} + \Delta Y_{\infty}(n - n_0) - \Delta Y_0 \exp(-\beta(n \pm n_0)^{\gamma})$

$(n + n_0)$ for molar volume, $(n - n_0)$ for all others

	Molar volume (cm3/gmol)	ln viscosity (cP)	Surface tension
n_0	-1.388524	-2.293981	0.264870
ΔY_0	a	a	a
$Y_{,0}$	0	57.8516	a
ΔY	a	a	0
β	0.183717	2.476409	2.511846
γ	0.753795	0.0112117	0.201325

[a] See Table 3

Table 2.4. Temperature-Dependent Parameters for Properties of *n*-Paraffins

$\Delta Y = A + B/T + C\ln T + DT^2 + E/T^2$ for $\ln\mu_L$

ΔY or $Y = A + BT + CT^2 + DT^3$ for V_L, σ

	Molar volume (cm3/gmol)		ln viscosity (cP)		Surface tension (dyne/cm)	
	ΔY_0	ΔY	ΔY_0	ΔY	ΔY_0	ΔY
A	8592.30	12.7924	-602.688	0.0290196	627.213	73.8715
B	-85.7292	0.0150627	77866.8	-241.023	-0.882888	-0.177123
C	0.280284	-130794×10^{-5}	198.006	0.0440959	0.00268188	1.54517×10^{-4}
D	-4.48451×10^{-4}	1.59611×10^{-4}	-4.18077×10^{-7}	-1.84891×10^{-7}	0	0
E			-2.49477×10^{6}	56561.7		
ΔT	0-300°C	0-300°C	0-300°C	0-300°C	0-150°C	0-150°C

2.4.2 Solid Phase (Catalyst)

Sabatier and Sanderson found in 1902 that methane can be obtained when hydrogen and carbon monoxide react over nickel or cobalt catalyst (Storch et al., 1951). Fischer and Tropsch in 1923 obtained a high yield of liquid products by using iron based alkali promoted catalyst. Process was later studied using iron, cobalt and nickel catalysts. First industrial scale and all pre and during WWII processes in Germany used cobalt based catalyst, 100Co:5ThO:8MgO:200Kieselguhr, because of its high activity. Due to the shortage in supply of Cobalt during WWII new iron based catalysts were developed. Ruhrchemie company developed a series of iron based catalysts, 100Fe:xCu:yK:zSiO2. South African commercial, ARGE, process still uses this type of a catalyst (x:y:z=4.3:4.1:25). Iron although less active is much cheaper and more easily available than cobalt. Srivastava et al. (1990) and Rao et al. (1992) reviewed various iron based FT catalysts. Nickel has been the most often used in combination with some other active component, such as cobalt. Ruthenium is the forth originally proposed Fisher-Tropsch